Title
Seismic Response Analysis of Highway Overcrossings Including Soil-Structure Interaction

Journal
Earthquake Engineering and Structural Dynamics, 31(11)

Authors
Zhang, Jian
Makris, Nicos

Publication Date
2002

Peer reviewed

SEISMIC RESPONSE ANALYSIS OF HIGHWAY OVERCROSSINGS INCLUDING SOIL-STRUCTURE INTERACTION

JIAN ZHANG[1] and NICOS MAKRIS[2]

Department of Civil and Environmental Engineering, U. C. Berkeley, CA 94720

SUMMARY

This paper presents a systematic procedure for the seismic response analysis of highway overcrossings. The study employs an elementary stick model and a more sophisticated finite element formulation to compute response quantities. All dynamic stiffnesses of approach embankments and pile groups are approximated with frequency-independent springs and dashpots that have been established elsewhere. A real eigenvalue analysis confirms the one-to-one correspondence between modal characteristics obtained with the three-dimensional finite element solutions and the result of the simpler stick-model idealization. A complex eigenvalue analysis yields modal damping values in the first six modes of interest and shows that modal damping ratios assume values much higher than those used by Caltrans. The validity of the proposed method is examined by comparing the computed time response quantities with records from the Meloland Road and Painter Street overcrossings located in southern and northern California respectively. The proposed procedure allows for inexpensive parametric analysis that examines the importance of considering soil-structure interaction at the end abutments and center bent. Results and recommendations presented by past investigations are revisited and integrated in comprehensive tables that improve our understanding on the dynamic characteristics and behavior of freeway overcrossings. The study concludes with a step-by-step methodology that allows for a simple, yet dependable dynamic analysis of freeway overcrossings, that involves a stick model and frequency-independent springs and dashpots.

KEY WORDS: dynamic analysis, highway bridges, earthquakes, soil-structure interaction.

INTRODUCTION

The motivation for this study did not originate from a lack of published material on the seismic response of freeway overcrossings but rather from an abundance of publications, the vast numbers of which present findings that are scattered, occasionally conflicting, and derived from

1. Graduate Student Researcher
2. Associate Professor

various methodologies that in many occasions have little in common. As a result, despite several existing recommendations (Werner 1994; Goel and Chopra 1997, among others) there is no established procedure that results in a dependable estimate of the seismic response of freeway overcrossings, partly because the findings of the below-mentioned studies have not been combined in a rational manner that will result in a systematic analysis procedure.

The seismic response of freeway overcrossings received distinct attention in the late 1980s. Maragakis and Jennings (1987) introduced the "stick model" enhanced with bilinear "springs" and "dashpots" at its support to study the motion of skew overpasses. Their model accounted for several practical difficulties such as the presence of elastomeric pads and the gap between the deck and the back wall. Werner et al. (1987) developed a system identification methodology to extract information from an array of strong-motion measurements that were recorded in the vicinity of the Meloland Road Overcrossing during the 1979 Imperial Valley earthquake. Their conclusions emphasized the ability of linear models to fit the measured response and the pronounced effects that the approach embankments and foundations have on the response of the bridge. Although their paper identifies relatively low values of modal damping for the bridge-foundation system ($\xi_i = 6\%$ to 8%), a later publication by Werner (1994) indicates modal damping ratios ranging from 19% to 26%. About the same time, Crouse et al. (1987) conducted experimental and analytical studies to determine the significance of soil-structure interaction on the response of a single span overcrossing with monolithic abutments on spread footings. The small displacement gradient generated from the ambient quick-release and forced-vibration tests resulted in small values of damping and large values of stiffness that are not representative under earthquake loading. The present paper revisits the problem of seismic response of highway overcrossings and proposes a systematic procedure to account for soil-structure interaction. Our goal is not to derive another isolated study, but rather to build on the work of others. Many past publications are used in this study to validate deformation levels, material parameters, and response quantities. Agreements between our results and those of other investigators further establish the dependability of the proposed procedure, while discrepancies in response quantities have been the motivation for the additional studies presented herein. This paper essentially builds on and extends the work of Wilson and Tan (1990b), Werner (1994), Goel and Chopra (1997), McCallen and Romstad (1994) and Makris et al. (1994).

The work of S. D. Werner and others on two-span short bridge overcrossings was summarized in a paper in an effort to evaluate Caltrans procedures for seismic response analysis of free-

way overcrossings (Werner 1994). That study underlined the significance of soil-structure interaction and offered selected recommended values on some modal parameters. Emphasis was given to the transverse response of the bridge. As in the Wilson and Tan (1990a) study, the Werner (1994) study did not provide any information on the embankment stiffnesses and damping along the longitudinal direction. Information on modal response quantities was limited to the first transverse mode only. Despite its limitations and occasional sweeping statements, the Werner (1994) study identifies several of the challenges associated with this problem. This study revisits the Werner (1994) paper by refining and extending several of the concepts advanced therein.

A comprehensive study that established the validity of the stick model was conducted by McCallen and Romstad (1994) who computed natural frequencies, mode shapes, and response time histories of the Painter Street Overcrossing using the two aforementioned numerical models. Both fixed and resilient foundation supports were considered and it was found that there is a one-to-one correspondence between the mode shapes predicted by the stick and the detailed finite element model. The McCallen and Romstad study indicated the substantial reduction in the transverse and longitudinal frequencies when realistic soil strains are considered; while in these two modes of vibration modal damping should be of the order of 20 to 30%. The levels of modal damping were concluded by McCallen and Romstad (1994) after a large number of trial and error iterations and comparisons of measured and computed responses at several bridge locations. The detailed finite element study by McCallen and Romstad (1994) that accounts for the resilience and dissipation at the center bent and end abutment involved the discretization of embankments and a large volume of the surrounding soil. Efforts to establish the validity of the stick model in estimating the seismic response of skew bridges have been also reported by Werner (1994).

Established values of kinematic response functions and dynamic stiffnesses of the approach embankments and pile foundations are used in this study to synthesize a simple dynamic model to estimate the dynamic response of freeway overcrossings. The numerical simulations that employ a simple stick model and a more sophisticated finite element model build on the work presented by McCallen and Romstad (1994). In contrast with the McCallen and Romstad study, the methodology presented in this paper adopts the substructure approach, where the kinematic response functions and dynamic stiffnesses are computed separately and subsequently are incorporated in a simple dynamic model where the mechanical behavior of each of its components can be calculated with any desired level of sophistication. The methodology to compute the kinematic response functions and dynamic stiffnesses of approach embankments is presented in the compan-

ion paper, whereas the methodology to compute the dynamic stiffnesses of pile groups has been summarized in the paper by Makris et al. (1994).

Lastly, the structural characteristics that we compute for the Painter Street Overcrossing are compared with those reported by Goel and Chopra (1997), who employed an equilibrium based approach to back-figure abutment stiffnesses at different levels of shaking. The follow-up work of Goel (1997) is also used to compare the estimated values of modal periods and damping ratios of the entire bridge-foundation system.

SOIL-STRUCTURE INTERACTION

Figure 1(a) shows the schematic of a typical two-span overcrossing with its approach embankments. During ground shaking the dynamic response of the deck is affected: (a) from the dynamic response of the embankments that support the end abutment and (b) from the dynamic response of the pile foundations at the center bent. The need to account for this interaction motivated finite element studies that involved the discretization of the bridge superstructure and a large volume of the embankments and supporting soil (Sweet 1993; McCallen and Romstad 1994 among others). Although such studies elucidated the significance of deck-abutment-embankment interaction, they do not provide direct information on the distinct mechanical characteristics of approach embankments and pile foundations and their influence on the dynamic response of the bridge structure. This might be a possible reason for the lack of practical procedures to account for soil-structure interaction when computing the seismic response of freeway overcrossings. This paper together with its companion paper (Zhang and Makris 2001) concentrates on addressing the issue of the importance of soil-structure interaction on the seismic response of freeway overcrossings and proposes a practical methodology to include its effect in association with simple bridge models.

Owing to its computational efficiency the substructure method is a popular approach to address the soil-foundation-superstructure problem (Tseng and Penzien 2000). Assuming linear soil-foundation-superstructure response, the analysis of the system can be performed in three consecutive steps as shown in Figure 1. First, find the motion at the end abutments and pile cap of the center bent in the absence of the bridge superstructure (the so-called foundation input motion), which includes translational as well as rotational components; second, determine the dynamic stiffnesses (frequency dependent springs and dashpots) associated with longitudinal, transverse, vertical, rocking and cross-horizontal-rocking oscillations of the embankments and pile groups;

third, compute the seismic response of the superstructure (deck and abutments) supported on springs and dashpots and subjected to the foundation input motion.

An earlier attempt to investigate the effect of soil-pile-structure interaction was presented by Makris et al. (1994). In that study the Painter Street Overcrossing was idealized with a plane six-degree-of-freedom lumped-parameter model, whereas the influence of the approach embankments was neglected. The limitations of the plane model restricted the analysis of the response only along the transverse direction. Despite its limitations, that study indicates some of the shortcomings that may result by neglecting the resilience of the pile foundations at the center bent and outlines a simple integrated procedure that one can follow in order to compute the stiffnesses and damping of pile foundations. The same procedure was adopted and extended in this study which examines the two-dimensional coupled longitudinal and transverse response of highway overcrossings. Figure 1 (bottom) shows the elevation and plan views of the model adopted in this study and the springs and dashpots that are proposed to approximate the interaction of the bridge superstructure with its foundation and the surrounding soil.

Dynamic Stiffnesses of Approach Embankments

The dynamic stiffnesses of approach embankments have been examined in the companion paper and for most practical purposes they can be replaced with frequency independent springs and dashpots.

Dynamic Stiffnesses of Pile Groups

The dynamic stiffnesses of a pile group, in any vibration mode, can be computed using the dynamic stiffnesses of a single pile in conjunction with the concept of superposition criterion, originally developed for static loads by Poulos (1968), and later justified for dynamic loads by Kaynia and Kausel (1982), Sanchez-Salinero (1983) and Roesset (1984). It can be used with confidence at least for groups with less than 50 piles. Dynamic interaction factors for various modes of loading are available in the form of non-dimensional graphs (Gazetas et al. 1991) and in some cases, closed form expressions derived from a beam on winkler foundation model in conjunction with simplified wave-propagation theory (Dobry and Gazetas 1988; Makris and Gazetas 1992).

Although the dynamic stiffnesses of pile groups are in general frequency dependent quantities, their low frequency values do not fluctuate appreciably with frequency and one can replace

them with frequency independent springs and dashpots (Zhang and Makris 2001). The stiffness matrix of a pile foundation is symmetric so that $K_{x\theta} = K_{\theta x} =$ moment at the pile cap for a positive unit displacement along the x direction. With the system of axis shown in Figure 1, a positive unit displacement along the x direction generates a negative moment. In contrast, a positive unit displacement in the y direction generates a positive moment so that $K_{y\theta} = K_{\theta y} > 0$. K_{θ} is the moment along the θ direction due to a unit rotation in this direction.

RESPONSE OF THE MELOLAND ROAD OVERCROSSING

Figure 2 shows the stick model (left) and the three-dimensional finite element model (right) of the Meloland Road Overcrossing in its deformed configuration. The stick model is a collection of beam elements with cross-section properties adjusted from geometric data without considering any cracked section reduction. The three-dimensional finite element model uses eight-node solid elements for the bridge superstructure. The bridge superstructure is supported at its center bent and at each end by the springs and dashpots schematically shown in Figure 1. The spring and dashpot values of the approach embankments have been estimated with the methodology presented in the companion paper, whereas the spring and dashpot values of the pile foundations have been estimated with the methodology presented in the paper by Makris et al. (1994) and is also included in the report by Zhang and Makris (2001). All values of interest are summarized in Table 1. The loops shown at the far ends of the bridge models in Figures 2 and 8 represent the deformed embankment springs as being plotted by ABAQUS.

During the numerical simulation, the Young's modulus of the beam elements on top of the column was artificially increased by three orders of magnitude to form a rigid link in order to prevent excessive deflections at the connection point between pier and deck in the stick model, (McCallen and Romstad 1994). Vertical excitations are not considered. In both models, the damping of the bridge deck and center bent is approximated with the Rayleigh damping approximation, where the parameters α and β are computed by assuming a 5% modal damping ratio in the first and the second modes. The Young's modulus of the concrete is assumed to be $E_c = 22\ GPa$. This value is approximately 80% of the value obtained from empirical expressions to account for the cracking that occurred during the earthquake. Similar cracked values for the Young's modulus of concrete in seismic response analysis of bridges have been reported by Douglas and Reid (1982, $E_c = 20 \sim 25\ GPa$) and Dendrou et al. (1985, $E_c = 20\ GPa$). The density of concrete is assumed 2400 kg/m^3.

TABLE 1. Spring and dashpot values that approximate the presence of the approach embankments and pile foundation of the Meloland Road Overcrossing. Values from this study are associated with the intensity of the 1979 Imperial Valley earthquake.

Parameters		1	2	3	4	5	6
Embankment + Pile Foundations	$K_x\ (MN/m)$	21+56	160*	91 (365)	107	/	607+49 (51+49)
	$K_y\ (MN/m)$	21+56	/	91 (365)	/	/	596+49
	$K_z\ (MN/m)$	78+356	418*	263 (1051)	/	/	/
	$C_x\ (MN \cdot s/m)$	1.5+4.5	/	/	/	/	/
	$C_y\ (MN \cdot s/m)$	1.5+4.5	/	/	/	/	/
	$C_z\ (MN \cdot s/m)$	3+28	/	/	/	/	/
Pile Foundation of Center Bent	$K_x, K_y\ (MN/m)$	260	/	254 (876)	/	1007	175
	$K_\theta\ (MN \cdot m/rad)$	7611	366	1888 (6509)	/	5696	/
	$K_{x\theta}\ (MN/rad)$	-409	/	/	/	/	/
	$K_{y\theta}\ (MN/rad)$	409	/	/	/	/	/
	$K_z\ (MN/m)$	887	/	550 (1898)	/	1460	/
	$C_x, C_y\ \ (MN \cdot s/m)$	6	/	/	/	/	/
	$C_z\ (MN \cdot s/m)$	25	/	/	/	/	/
Note	1. This study ($G = 2.0\ MPa$ and $\eta = 0.52$ for embankment soil) 2. Wilson and Tan 1990a (* embankment only, no piles and $G = 7.2\ MPa$ is used for embankment soil) 3. Douglas, Maragakis and Vrontinos 1991 (values in parenthesis are the optimal values identified from dynamic tests) 4. Werner 1994 (fixed boundary condition at the base of pier) 5. Maragakis, Douglas and Abdel-Ghaffar 1994 (values are from dynamic tests) 6. Caltrans: Method A (Method B)						

Eigenvalue Analysis

Eigensolutions were performed for the stick model and three-dimensional finite element model using the commercially available software ABAQUS. Figure 2 compares the first six modes and modal frequencies of the stick model and three-dimensional finite element model, and indicates a one-to-one correspondence between the two models. The natural frequencies of the stick model are also in good agreement with that of the three-dimensional finite element model.

While modal frequencies are directly estimated by solving the real eigenvalue problem of some structural idealization of the bridge-foundation system having mass matrix, $[M]$, and stiffness matrix, $[K]$, the estimation of the modal damping ratios appears to be a less straightforward procedure. The majority of modal damping ratios of bridges published in the literature have been back-figured by processing recorded data with system identification algorithms (Wilson 1986; Werner et al. 1987; Wilson and Tan 1990b; Werner 1994; and Goel 1997 among others). Although more recent multi-input-multi-output system identification algorithms appear to be more efficient than older single-input-single-output algorithms, the relevance of the reported values is strongly associated with the sophistication of the adopted structural model and the quality of the recorded data. In some occasions modal damping values appreciably larger than those identified were recommended (Werner 1994).

In an effort to calibrate finite element results, McCallen and Romstad (1994) initially assigned a uniform modal damping ratio, $\xi_j = 5\%$, to the first six modes of the Painter Street Overcrossing. Subsequently, after conducting a large number of trial and error iterations and comparisons of recorded and computed responses of the bridge, they reassigned much larger values of modal damping to selected modes in order to approximate satisfactorily the recorded responses. In this study the modal damping ratios of the bridge foundation system are computed by solving for the complex eigenvalues of the homogeneous equation

$$[M]\{\ddot{u}\} + [C]\{\dot{u}\} + [K]\{u\} = 0 \tag{1}$$

where $[M]$, $[C]$, and $[K]$ are the mass, damping, and stiffness matrices of the bridge-foundation idealization shown in Figure 1.1 and $\{u\}$ is the free vibration response vector

$$\{u\} = \{\phi\} e^{i\Omega t} \tag{2}$$

In equation (2), Ω is the complex characteristic value and $\{\phi\}$ is the associated characteristic vector. This complex eigenvalue approach is well known in the literature and was given a critical review by Veletsos and Ventura (1986). The damping matrix, $[C]$, is constructed by adopting the concept of Rayleigh damping for the bridge superstructure and appending the pre-identified lumped dashpots at the locations where the superstructure interacts with its foundation. Following this approach we assign a 5% modal damping ratio at the first and second modes of the undamped idealized model (bridge deck with springs) and add the damping constants, c_{ij}, identified in the companion paper (Zhang and Makris 2001, for the embankments) and in the paper by Makris et al. (1994, for the pile groups), that represent the presence of the embankments and pile founda-

tions. With this superposition the nonclassical damping matrix, $[C]$, of the bridge-foundation system assumes the form

$$[C] = \alpha[M] + \beta[K] + [c_{ij}] \tag{3}$$

The matrix $[c_{ij}]$ is assembled in the same way as the stiffness matrix $[K]$ of the undamped superstructure so that the lumped dashpots c_{ij} are assigned to the correct degrees of freedom. Substitution of (2) in (1) yields

$$(-\Omega^2[M] + i\Omega[C] + [K])\{\phi\} = 0 \tag{4}$$

which is a standard polynomial eigenvalue problem. The roots of this polynomial are the complex characteristic values Ω_j that were evaluated with MATLAB (1997). The relation between Ω_j with the modal frequencies, ω_j, and modal damping ratios, ξ_j $(j = 1, 2, ...N)$ is determined from the associated equation of a single-degree-of-freedom oscillator. Interpreting Ω_j as the frequency domain parameter one may determine

$$\Omega_j = \pm\sqrt{\omega_j^2 - \xi_j^2\omega_j^2} + i\xi_j\omega_j \tag{5}$$

After solving for ω_j and ξ_j,

$$\omega_j = \sqrt{\Omega_{jR}^2 + \Omega_{jI}^2} \tag{6}$$

$$\xi_j = \frac{\Omega_{jI}}{\omega_j} \tag{7}$$

in which Ω_{jR} and Ω_{jI} are the real and imaginary parts of the characteristic value Ω_j, respectively.

The stick model used in the real eigenvalue analysis consists of 354 degrees of freedom for Meloland Road Overcrossing. In order to bypass the problem of computing and interpreting the complex eigenvalues of such large matrices, a reduced-order stick model was developed with fewer degrees of freedom. Sensitivity studies indicated that the modal characteristics of the first ten modes are virtually insensitive to the exact number of elements of the reduced-order stick model. Two reduced-order stick models that consist of 228 and 300 degrees of freedom (d.o.f) respectively yield nearly identical results as indicated in Table 2.

TABLE 2. Modal frequencies, ω_j (rad/s), and damping ratios, ξ_j (%), of the Meloland Road Overcrossing

Modes	Eigenvalues (rad/s)				1		2		3		4	5	
	Model A	Model B	Model C	Model D	ω_j	ξ_j	ω_j	ξ_j	ω_j	ξ_j	ω_j	ω_j	ξ_j
1st transverse	12.320	12.647	12.440 (12.441)	$13.519 + 2.5771i$ $(13.702 + 2.7333i)$	13.8 (13.8)	18.7 (18.7)	15.5	7.2	14.3~15.7	6.6~12.7	15.6	16.3	19~26
longitudinal	16.044	17.913	17.882 (17.884)	$16.001 + 11.047i$ $(16.221 + 11.104i)$	19.4 (19.4)	56.8 (56.8)					16.7		
1st vertical (antisymmetric)	21.405	22.460	21.911 (21.921)	$21.073 + 1.746i$ $(21.252 + 1.888i)$	21.1 (21.2)	8.3 (8.3)					17.5		
torsion about vertical axis	24.521	25.105	23.823 (23.824)	$0.0 + 17.942i$ $(0.0 + 17.962i)$	17.9 (18.0)	100 (100)	Critically Damped Mode						
2nd transverse/torsion about longitudinal axis	26.996	25.340	25.096 (25.087)	$25.778 + 7.570i$ $(26.830 + 8.010i)$	26.9 (26.9)	28.2 (28.2)							
2nd vertical (symmetric)	30.724	26.515	26.496 (26.526)	$28.153 + 2.895i$ $(28.187 + 2.900i)$	28.3 (28.3)	10.2 (10.2)	28.7	5.8	27.4~29.9	3.1~7.4	27.6		
Note	A: Undamped original 3D FEM model B: Undamped original stick model C: Undamped reduced stick model with 300 d.o.f and (228 d.o.f) respectively D: Damped reduced stick model with 300 d.o.f and (228 d.o.f) respectively 1: This study 2: Werner, Beck, and Levine 1987; 3: Wilson & Tan 1990b 4: Gates 1993 5: Werner 1994												

Table 2 presents the first six real eigenvalues of the Meloland Road Overcrossing that have been computed with the 3D finite element model of the undamped bridge (column A), the original stick model of the undamped bridge (column B, d.o.f=354), the reduced-order stick model of the undamped bridge (column C, d.o.f=300 and 228 respectively), and the first six complex eigenvalues of the reduced-order stick model of the damped bridge (column D, d.o.f=300 and 228 respectively). The corresponding damping ratios computed with this study are shown in column 1, next to other values reported in the literature.

The values shown in Table 2 indicate that the reduced-order stick model in association with the complex eigenvalue analysis yield valuable information on the free vibration characteristics of the bridge.

- The computed modal damping ratios, ξ_j, are much larger than the 5% modal damping assumed by Caltrans.
- The computed first modal damping ratio, $\xi_1 = 18.7\%$, which in this case corresponds to the first transverse mode with the deck bending away from the undeformed configuration, is in agreement with the low end of damping values along the transverse mode that are reported by Werner (1994). The values of first modal damping reported by Werner (1994) are appreciably larger than the value by the same and other investigators during earlier studies on the same bridge (Werner et al. 1987).
- The computed second modal damping $\xi_2 = 56.8\%$ is unusually high. However, our confidence in this value originates from the straight configuration of the deck and its integral abutments which are mobilizing a large volume of soil with high damping. Indirect evidence that this high damping value might be realistic is provided by the inability of system identification studies to detect modal characteristics along the longitudinal mode of vibration.
- The modal damping associated with the third mode (1st vertical, antisymmetric, $\xi_3 = 8.3\%$) is lower than the modal damping associated with the transverse and the longitudinal modes that involve more soil participation.
- The torsional mode about the vertical axis is critically damped. Since the modes are decoupled the modal damping of the torsional mode can be estimated by assuming that the deck is a single-degree-of-freedom structure with length, L, and linear mass density, m, that rotates about

the center bent and its motion is resisted at the two ends by the transverse springs and dashpots of the embankments indicated in Table 1. With this idealization, the equation of motion for torsion about the vertical axis is

$$I_0\ddot{\theta} + \frac{1}{2}C_x L^2\dot{\theta} + \frac{1}{2}K_x L^2\theta = 0 \tag{8}$$

where $I_0 = \frac{1}{12}mL^3$ is the moment of inertia of the deck about the vertical axis. Using the standard real valued procedure (Chopra 1995) or the complex formulation given by equations (6) and (7) one concludes that $\omega_5 = \sqrt{\frac{6K_x}{mL}} \approx 26.2\ rad/s$ and $\xi_5 = (3C_x)/(\sqrt{6K_x mL}) \approx 1.0$.

- The computed fifth modal damping $\xi_5 = 28.6\%$ also assumes a high value, probably due to the explanation offered above, since this mode involves the transverse motion of the deck as well as torsional motion of deck about the longitudinal axis.
- The good agreement between the values reported for the first and sixth natural frequencies of the MRO by various investigators is worth mentioning.

Time History Analysis

Figures 3 to 5 plot total acceleration, relative velocity, and displacement time histories of the bridge response at selected locations. The analysis shown in these figures investigates the sensitivity of the bridge response to the support motion. The first column shows the recorded motions. The second column (case 1) shows computed response quantities by using as a support motion at the end abutments the crest motions computed using Equation (14) in the companion paper. The third column (case 2) shows the computed response quantities by using as a support motion at the center bent and the end abutments the free-field motion. The last column (case 3) shows computed response quantities by using as a support motion at the end abutments the recorded crest motions. All simulated responses are obtained by implementing the spring and dashpot values that have been evaluated with the approximate methods advanced in the companion paper.

Figure 3 compares the computed response with the records of channel 7, which is located at mid-span of the bridge deck (see Figure 6 of the companion paper). The case where the recorded crest motions is used as support motions yields the best overall predictions. The acceleration and the deck drift are predicted with errors less than 8%, while the relative velocity is underestimated by 26%. When the computed crest motions are used as support motions, the peak acceleration is

overestimated by 27% while the deck drift and the relative velocity is predicted with marginal discrepancies. Figure 4 compares the computed response with the records of channel 8. When the free-field motions are used as support motions the discrepancies between records and predictions are of the order of 70% or more for relative velocities and relative displacements. When the computed crest motions are used as support motions the peak acceleration is overestimated by 50% while the deck drift history contains higher frequencies than the recorded. Similar trends can be observed in Figure 5, which compare the computed responses with the records of channel 13. The results shown in Figures 3 to 5 indicate the significance of considering the amplified support motions at the crest of the embankments. More comparisons between recorded and computed time histories are offered in the report by Zhang and Makris (2001)

Our parametric analysis proceeds by analyzing the bridge response when different support idealizations are considered. Figure 6 shows three idealizations of interest: (a) monolithic abutments and viscoelastic foundation at the center bent, (b) viscoelastic embankments and monolithic support at the center bent, and (c) viscoelastic embankments and elastic support at the center bent. The sensitivity of the bridge responses to the resilience and dissipation of the bridge supports is investigated in Figure 7, which compares the response quantities against the records of channel 7. The first column in Figure 7 shows the recorded motions. The second column shows computed response quantities by assuming monolithic abutments and viscoelastic foundation at the center bent. It examines the effect of neglecting the resilience and dissipation at the abutments. It is shown that in this case the response is more high frequency with overestimated peak acceleration. The third column examines the effect of neglecting the resilience and dissipation of the pile foundation at the center bent. The last column examines the effect of neglecting the dissipation of the pile foundation at the center bent. All simulated response are subjected to the recorded motions at the crest of the embankment and the free-field and should be compared with the last column of Figure 3. The case of a rigid support at the center bent (third column) results in the smaller drifts, while the case of neglecting the dissipation of the pile foundations (Goel and Chopra 1997) yields comparable results when it is included.

RESPONSE OF THE PAINTER STREET OVERCROSSING

Figure 8 shows the stick model (left) and three-dimensional finite element model (right) of the Painter Street Overcrossing in its deformed configurations. Again, the stick model is a collection of beam elements with cross-section properties adjusted from geometric data without consid-

ering any cracked section reduction. While it is not shown in Figure 8 the beam elements are joined following the skew configuration of the bridge that results in coupling of the vibration modes. The three-dimensional finite element model uses eight-node solid elements for the bridge structure. The bridge superstructure is supported at its center bent and both ends by the springs and dashpots schematically shown in Figure 1 — their values being estimated separately in the companion paper and summarized in Table 3 (column 1), along with selected values reported in literature (columns 2 to 5).

TABLE 3. Spring and dashpot values that approximate the presence of the embankments and pile foundations of the Painter Street Overcrossing. Values from this study are associated with the intensity of the 1992 Petrolia earthquake.

Parameters		1	2	3	4	5
Embankment + Pile Foundations	$K_x\ (MN/m)$	137+180	201*	851+105	117~438+	810+105 (68+105)
	$K_y\ (MN/m)$	137+180	/	815+105	146~1458+	876+105
	$K_z\ (MN/m)$	582+773	564*	∞	/	/
	$C_x\ (MN \cdot s/m)$	9+9	/	/	/	/
	$C_y\ (MN \cdot s/m)$	9+9	/	/	/	/
	$C_z\ (MN \cdot s/m)$	17+56	/	/	/	/
Pile Foundation of Center Bent	$K_x, K_y\ (MN/m)$	321	/	140	/	140
	$K_\theta\ (MN \cdot m/rad)$	5254	/	/	/	/
	$K_{x\theta}\ (MN/rad)$	-354	/	/	/	/
	$K_{y\theta}\ (MN/rad)$	354	/	/	/	/
	$K_z\ (MN/m)$	982	/	∞	/	/
	$C_x, C_y\ \ (MN \cdot s/m)$	5	/	/	/	/
	$C_z\ (MN \cdot s/m)$	20	/	/	/	/
Note	1. This study ($G = 8.0\ MPa$ and $\eta = 0.50$ for embankment soil) 2. Wilson and Tan 1990a (* embankment only, no piles) 3. McCallen and Romstad 1994 4. Goel and Chopra 1997(+ embankment and piles) 5. Caltrans 1989 Method A (Method B)					

Vertical excitations are not included during the analysis. In both models, the damping of the bridge superstructure is approximated with the Rayleigh damping approximation, where the

parameters α and β are computed by assuming a 5% modal damping ratio in the first and the second modes. The Young's modulus of the concrete is assumed to be 22GPa. This value is approximately 80% of the value obtained from empirical expressions to account for the cracking that occurred during the earthquake. The density of concrete is 2400 kg/m^3.

Eigenvalue Analysis

Eigensolutions were performed for the stick model and three-dimensional finite element model using the commercially available software ABAQUS. Figure 8 compares the first six natural modes and frequencies of the stick model and the three-dimensional finite element model.

There is a one-to-one correspondence between the mode shapes predicted by the stick model and three-dimensional finite element model. The natural frequencies of the stick model are also in good agreement with that of the three-dimensional finite element model. The first values shown are those computed by adopting the converged soil properties during the strong 1992 Petrolia earthquake. The values shown in the parenthesis are those reported by McCallen and Romstad (1994). They are 50% higher than the values computed in this study. Part of the reason for these discrepancies is the six times larger embankment stiffnesses they used in their study.

Modal damping ratios are estimated with the complex eigenvalue procedure presented in the section associated with the analysis of the Meloland Road Overcrossing. Similarly, a reduced-order stick model was developed with fewer degrees of freedom in order to bypass the problem of computing and interpreting the large number of complex eigenvalues resulting from the original stick model which consists of 618 degrees of freedom. Table 4 presents the first six eigenvalues of the Painter Street Overcrossing that have been computed with the three-dimensional (3-D) finite element model of the undamped bridge (column A), the original stick model of the undamped bridge (column B), the reduced-order stick model of the undamped bridge (column C); and the first six complex eigenvalues of the reduced-order stick model of the damped bridge. Damping ratios computed with this study are shown in column 1 next to other values reported in the literature. Selected observations from the modal values indicated in Table 4 are:

- Due to the skew configuration, there is strong coupling of modes involved in the eigenvalue analysis.

TABLE 4. Modal frequencies, ω_j (rad/s), and damping ratios, ξ_j (%), of the Painter Street Overcrossing

Modes	Eigenvalues (rad/s)				1		2		3		4	
	Model A	Model B	Model C	Model D	ω_j	ξ_j	ω_j	ξ_j	ω_j	ξ_j	ω_j	ξ_j
1st transverse/antisymmetric vertical	14.514	11.162	11.364 (11.587)	$11.490 + 1.040i$ $(11.730 + 1.116i)$	11.5 (11.8)	9.0 (9.5)	20.7	20	11.0~17.9	5.6~8.5	10.3	16.6
antisymmetric vertical/torsion about vertical axis	17.593	14.409	14.578 (14.751)	$14.683 + 0.984i$ $(14.863 + 1.006i)$	14.7 (14.9)	6.7 (6.8)	16.9	3				
torsion about vertical axis/ symmetric vertical	18.410	16.366	16.365 (16.366)	$16.527 + 0.962i$ $(16.524 + 0.972i)$	16.6 (16.6)	5.8 (5.9)	25.1	3				
symmetric vertical/longitudinal	23.562	20.691	20.808 (20.994)	$21.075 + 1.761i$ $(21.370 + 1.809i)$	21.1 (21.4)	8.3 (8.4)	32.9	5				
longitudinal	26.641	21.545	20.938 (21.265)	$20.176 + 10.383i$ $(20.394 + 10.395i)$	22.7 (22.9)	45.8 (45.4)	29.6	30				
2nd transverse/torsion about longitudinal axis	32.233	31.156	22.052 (22.532)	$23.754 + 4.096i$ $(24.236 + 4.302i)$	24.1 (24.6)	17.0 (17.5)	41.5	5				
Note	A: Undamped original 3D FEM model B: Undamped original stick model C: Undamped reduced stick model with 174 d.o.f and (138 d.o.f) respectively D: Damped reduced stick model with 174 d.o.f and (138 d.o.f) respectively 1: This study 2: McCallen and Romstad 1994 3: Goel 1997 4. Price and Eberhard 1998											

- The computed modal damping ratio, ξ_j, are larger than the 5% modal damping assumed by Caltrans, however, the first three modal damping ratios are not as high as the modal damping ratios computed for the straight (unskewed) Meloland Road Overcrossing. This might be partly due to the strong participation of the vertical mode in the Painter Street Bridge that is associated with less damping.
- The computed first modal damping, $\xi_1 = 9\%$ is approximately half the value that McCallen and Romstad (1994) needed to match the recorded data. However, it is in agreement with the high-end of the modal damping range identified by Goel (1997).
- The longitudinal mode (that was the second mode for the Meloland Road Overcrossing) has been pushed down to the fifth mode. Interestingly, the complex eigenvalue analysis advanced in this study is able to capture the high damping, $\xi_5 = 46\%$, associated with this mode. As was indicated during the analysis of the modal properties of the Meloland Road Overcrossing, in which $\xi_2 = 56.5\%$ (longitudinal mode), the longitudinal mode mobilize a large volume of soil with high damping.
- The procedure advanced in this study, where the appropriate values of G and η of the soil embankments are established with the kinematic response analysis, yields a first natural frequency that is in very good agreement with the values reported by Goel (1997) and Price and Eberhard (1998).

Time History Analysis

Figures 9 and 10 plot total acceleration, relative velocity, and displacement time histories of the bridge response at selected locations. The analysis shown in these figures investigates the sensitivity of the bridge response to the foundation input motion. The first column shows the recorded motions. The second column (case 1) shows computed response quantities by using as a support motion at the end abutments the crest motions computed using eq. (14) of the companion paper. The third column (case 2) shows the computed response quantities by using as a support motion at the center bent and end abutments the free-field motion. The last column (case 3) shows computed response quantities by using as a support motion at the end abutments the recorded crest motions.

Figure 9 compares the computed responses with the records of channel 4. The case where the recorded crest motions are used as support motions (last column) yields invariably the most

favorable prediction. When the free-field motions are used as support motions, the bridge response shown along the third column is substantially underestimated, since it has not experienced the amplification that the embankments induce at the two ends. When the computed crest motions are used as support motions the peak accelerations are predicted with marginal discrepancies; however, deck drifts are underestimated by 22% with a time history that exhibits higher frequencies than the recorded. Figure 10 which compares the computed response with the records of channel 7, indicates similar trends. When the free-field motions are used as support motions the discrepancies between records and predictions are of the order of 40% or more, for relative velocities and relative displacements. When the computed crest motions are used as input, the computed responses are as good as when the recorded crest motions are used. Additional comparisons between recorded and computed time histories are offered in the report by Zhang and Makris (2001).

The sensitivity of the bridge response to the resilience and dissipation of the bridge supports is investigated in Figures 11 and 12, which plot total acceleration, relative velocity, and displacement time histories. Again the first column shows the recorded motion for convenience. The second column plots the computed response quantities by assuming that the abutments are monolithic supports and soil-structure-interaction happens only at the foundation of the center bent (case (a) of Figure 6). The third column plots the computed response quantities by considering soil-structure-interaction at the end abutments and by assuming a monolithic support at the center bent (case (b) of Figure 6). The fourth column plots the computed response quantities by neglecting the dissipation of the pile foundation at the center bent. In all cases the free-field motions were induced at the foundation of the center bent and the recorded crest motions were induced at the end abutments.

Figure 11 compares the computed responses with the records of channel 4. It indicates that the flexibility of the pile foundation of the center bent is appreciably affecting the response, whereas the associated damping has less important effects. Neglecting the flexibility and damping of the end abutments results to a more high-frequency acceleration response. Figure 12, which shows computed responses at the mid-span, indicates the similar trends. More specifically, the results obtained by neglecting the damping of the pile foundation at the center bent are comparable to the results obtained when damping is included, a result that confirms the validity of the assumption adopted by Goel and Chopra (1997). These trends suggest that in this case the damp-

ing of the pile foundation at the center bent has marginal effects; whereas the flexibility of the pile foundations has an appreciable effect and has to be included.

OUTLINE OF PROPOSED PROCEDURE

The two case studies presented in this paper confirmed the validity of a step-by-step procedure to estimate the seismic response of freeway overcrossings. The study shows that the stick model used by Caltrans when enhanced with realistic springs and dashpots at its supports can yield dependable estimates of the seismic response of freeway overcrossings.

Step 1. Compute the kinematic response function of the approach embankments as outlined in the companion paper, after establishing the converged values of the equivalent linear soil parameters, G and η.

Step 2. Compute the embankment crest response by amplifying the free-field motion with the kinematic response functions obtained in step 1.

Step 3. Compute the frequency-independent spring and dashpot values of the approach embankment using the values of G and η established in step 1, as shown in the companion paper.

Step 4. Compute the frequency-independent spring and dashpot values of the pile groups at the abutments and the center bent as outlined in the paper by Makris et al. (1994).

Step 5. Construct a stick model of the bridge enhanced with the transverse and longitudinal spring and dashpot values computed in steps 3 and 4.

Step 6. Compute the two-dimensional dynamic response of the model constructed in step 5 (see Figure 1) subjected to the free-field motions at the center bent and the crest motions at the abutment ends computed in step 2.

CONCLUSIONS

The free-vibration and earthquake responses of two instrumented bridges are examined in this paper with a reduced-order stick model and a more detailed three-dimensional finite element model. Either model in this study was enhanced with the springs and dashpots established in the companion paper to account for the presence of the approach embankments and pile foundations. Our analysis revealed distinguishable trends that lead to the following conclusions:

- The reduced-order stick model yields comparable modal parameters and seismic response characteristics to the more detailed three-dimensional finite element model. It is capable to capture the dynamic characteristics of a skewed overcrossing that exhibits strong coupling of its vibration modes.
- The modal damping ratios, ξ_j, of either the straight Meloland Road Overcrossing and the skewed Painter Street Overcrossing are much larger than the 5% modal damping ratios assumed by Caltrans.
- The first mode of the straight Meloland Road Overcrossing is the transverse mode; whereas, for the skewed Painter Street Overcrossing, it is the coupled transverse/first antisymmetric vertical mode.
- The first modal damping ratio of the Meloland Road Overcrossing is of the order of 20%; whereas, for the Painter Street Overcrossing, it is of the order of 10%. The smaller amount of the first modal damping in the skewed Painter Street Overcrossing is because the transverse mode is coupled with the first antisymmetric vertical mode that is lightly damped.
- The longitudinal mode emerges as the second mode for the straight Meloland Road Overcrossing; whereas, in the skewed Painter Street Overcrossing, it is pushed down to the fifth place. In both cases the modal damping ratio along the longitudinal direction is of the order of 50%.
- Vertical vibration modes exhibit smaller damping ratios (8% to 10%).
- The torsional mode of the straight and symmetric overcrossings is highly damped. For the particular case of the Meloland Road Overcrossing, the torsional mode (4th mode) was critically damped, $\xi_4 \approx 100\%$. In contrast, in the case of the skewed Painter Street Overcrossing the torsional mode is coupled with the symmetric vertical mode and the modal damping was as low as $\xi_3 \approx 6\%$.
- Time history analysis shows that the amplified crest motions of the approach embankments have an appreciable effect on the bridge response and should not be neglected. When the computed crest motions are used as support motions at the abutments the prediction of the response is far superior than when one uses the free-field motions.
- Parametric studies that examine the effect of different support idealizations indicate that neglecting the resilience of the foundation of the center bent yields unrealistic small drifts, while neglecting the dissipation of the foundation of the center bent has a marginal effect.

In summary, in view of the strong effect of soil-structure interaction, it is concluded that the earthquake response of highway overcrossings can be realistically estimated with the stick model used by Caltrans provided that (a) it is enhanced with the springs and dashpots established in the companion paper and (b) it is subjected at its end abutments to the amplified crest motions.

ACKNOWLEDGEMENTS

Partial financial support for this study was provided by the National Science Foundation under Grant CMS-9696241. The valuable input and comments of Dr. Tim Delis are appreciated.

REFERENCES

1. CALTRANS (1989), *Bridge Design Aids 14-1*, California Department of Transportation, Sacramento, CA.

2. Chopra, A. K. (1995), *Dynamics of Structures: theory and applications to earthquake engineering*, Prentice Hall, Englewood Cliffs, NJ.

3. Crouse, C. B., Hushmand, B., and Martin, G. R. (1987), "Dynamic soil-structure interaction of single-span bridge", *Earthquake Engineering and Soil Dynamics,* Vol. 15, pp. 711-729.

4. Dendrou, B., Werner, S. D., and Toridis, T. (1985), "Three-dimensional response of a concrete bridge system to traveling seismic waves", *Computers & Structures,* Vol. 20, pp. 593-603.

5. Dobry, R. and Gazetas, G. (1988), "Simple method for dynamic stiffness and damping of floating pile groups", *Geotechnique*, Vol. 38, pp. 557-574.

6. Douglas, B. M. and Reid, W. H. (1982), "Dynamic tests and system identification of bridges", *Journal of the Structural Division*, ASCE, 108, ST10, pp.2295-2312.

7. Douglas, B. M., Maragakis, E., and Vrontinos, S. (1991), "Parameter identification studies of the Meloland Road Overcrossing", *Proc. Pacific Conference on Earthquake Engineering*, Auckland, New Zealand,Vol. 1, pp. 105-116.

8. Gazetas, G., Fan, K., Kaynia, A., and Kausel, E. (1991), "Dynamic interaction factors for floating pile groups", *Journal of Geotechnical Engineering,* ASCE, Vol. 117, No. 10, pp. 1531-1548.

9. Gates, J. H. (1993), "Dynamic field response studies and earthquake instrumentation of the Meloland Road Overcrossing", *Structural Engineering in Natural Hazards Mitigation: Proc. of Papers Presented at the Structures Congress'93*, Vol.1, pp.343-348, ASCE, New York, NY.

10. Goel, R. K. (1997), "Earthquake behavior of bridges with integral abutments", *Proc. of the National Seismic Conference on Bridges and Highways: Progress in Research and Practice*, pp. 149-159, Sacramento, CA.

11. Goel, R. K., and Chopra, A. K. (1997), "Evaluation of bridge abutment capacity and stiffness during earthquakes", *Earthquake Spectra,* Vol. 13, No. 1, pp. 1-23.

12. Kaynia, A. M. and Kausel, E. (1982), "Dynamic stiffness and seismic response of sleeved piles", *Report No. R80-12,* MIT, Cambridge, MA.

13. Makris, N. and Gazetas, G. (1992),"Dynamic pile-soil-pile interaction Part II: Lateral and seismic response", *Earthquake Engineering and Structural Dynamics*, Vol. 21, No. 2, pp. 145-162.

14. Makris, N., Badoni, D., Delis, E. and Gazetas, G. (1994),"Prediction of observed bridge response with soil-pile-structure interaction", *Journal of Structural Engineering*, Vol. 120, No. 10, pp. 2992-3011.

15. Maragakis, E. A., and Jennings, P. C. (1987), "Analytical models for the rigid body motions of skew bridges", *Earthquake Engineering and Structural Dynamics,* Vol. 15, No. 8, pp. 923-944.

16. Maragakis, E., Douglas, B. M., and Abdel-Ghaffar, S. M. (1994), "An equivalent linear finite element approach for the estimation of pile foundation stiffnesses", *Earthquake Engineering & Structural Dynamics*, 23, 10, pp. 1115-1124.

17. MATLAB (1997), Mathworks Inc., Natick, MA.

18. McCallen, D. B., and Romstad, K. M. (1994), "Analysis of a skewed short-span, box-girder overpass", *Earthquake Spectra,* Vol. 10, No. 4, pp. 729-755.

19. Poulos, H. G. (1968), "Analysis of the settlement of pile groups", *Geotechnique*, Vol. 18, No.4, pp. 449-471.

20. Price, T. E. and Eberhard, M. O. (1998), "Efficient procedure for modeling the transverse seismic response of bridge embankments", *Proc., Sixth U.S. National Conference on Earthquake Engineering*, Earthquake Engineering Research Inst., Oakland, CA.

21. Roesset, J. M., and Angelides, D. (1980), "Dynamic stiffness of piles", *Numerical methods in offshore piling*, Institution of Civil Engineers, London, pp. 75-82.

22. Sanchez-Salinero, I. (1983), "Dynamic stiffness of pile groups: approximate solutions", *Geotech. Engrg. Report No. GR83-5,* University of Texas, at Austin, TX.

23. Sweet, J. (1993), "A technique for nonlinear soil-structure interaction", *Rep. CAI093-100,* Sacramento, California.

24. Tseng, W.-S., and Penzien, J. (2000), "Soil-Foundation-Structure Interaction", *Bridge Engineering Handbook* (Chapter 42), editors: Chen, W.-F. and Duan, L., CRC Press, Boca Raton, FL.

25. Veletsos, A. S. and Ventura, C. E. (1986), "Modal analysis of non-classically damped linear systems", *Earthquake Engineering and Structural Dynamics,* Vol. 14, pp. 217-243.

26. Werner, S. D., Beck, J. L., and Levine, M. B. (1987), "Seismic response evaluation of Meloland road overpass using 1979 Imperial valley earthquake records", *Earthquake Engineering and Structural Dynamics,* Vol. 15, pp. 249-274.

27. Werner, S. D. (1994), "Study of Caltrans' seismic evaluation procedure for short bridges", *Proc. 3rd Annual Seismic Research Workshop*, California Department of Transportation, Sacramento, California.

28. Wilson, J. C. (1986), "System identification of the seismic response of a highway bridge", *Proc., 8th European Conference on Earthquake Engineering,* Vol. 3, pp. 17-24.

29. Wilson, J. C., and Tan, B. S. (1990a), "Bridge abutments: formulation of simple model for earthquake response analysis", *Journal of Engineering Mechanics,* Vol. 116, No. 8, pp. 1828-1837.

30. Wilson, J. C., and Tan, B. S. (1990b), "Bridge abutments: accessing their influence on earthquake response of Meloland Road Overpass", *Journal of Engineering Mechanics,* Vol. 116, No. 8, pp. 1838-1856.

31. Zhang, J., and Makris, N. (2001), *Seismic response analysis of highway overcrossings including soil-structure interaction*, PEER-2001/02, Pacific Earthquake Engineering Research Center, University of California, Berkeley.

32. Zhang, J., and Makris, N. (2001), "Kinematic response functions and dynamic stiffnesses of bridge embankments", *Earthquake Engineering and Structural Dynamics* (Companion Paper).

FIGURE LEGENDS

Figure 1. General procedure for seismic soil-foundation-superstructure interaction

Figure 2. First six natural frequencies and modes computed by stick model (left) and 3D FEM model (right) of Meloland Road Overcrossing

Figure 3. Records of channel 7 and predictions of Meloland Road Overcrossing response considering different support motions

Figure 4. Records of channel 8 and predictions of Meloland Road Overcrossing response considering different support motions

Figure 5. Records of channel 13 and predictions of Meloland Road Overcrossing response considering different support motions

Figure 6. Bridge models with different support idealizations

Figure 7. Records of channel 7 and predictions of Meloland Road Overcrossing response considering different support idealizations

Figure 8. First six natural frequencies and modes computed by stick model (left) and 3D FEM model (right). Values in parentheses are those reported by McCallen and Romstad (1994)

Figure 9. Records of channel 4 and predictions of Painter Street Overcrossing response considering different support motions

Figure 10. Records of channel 7 and predictions of Painter Street Overcrossing response considering different support motions

Figure 11. Records of channel 4 and predictions of Painter Street Overcrossing response considering different support idealizations

Figure 12. Records of channel 7 and predictions of Painter Street Overcrossing response considering different support idealizations

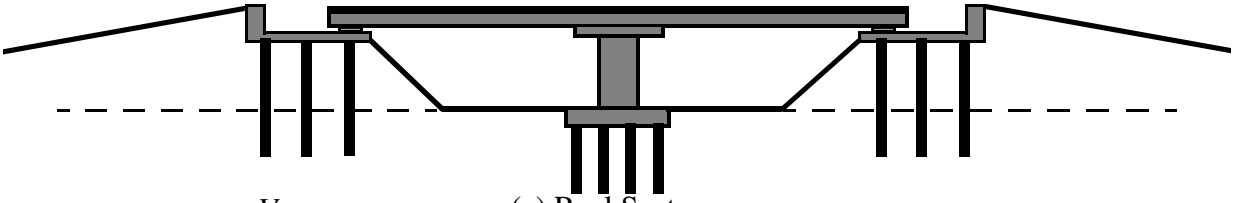

(a) Real System

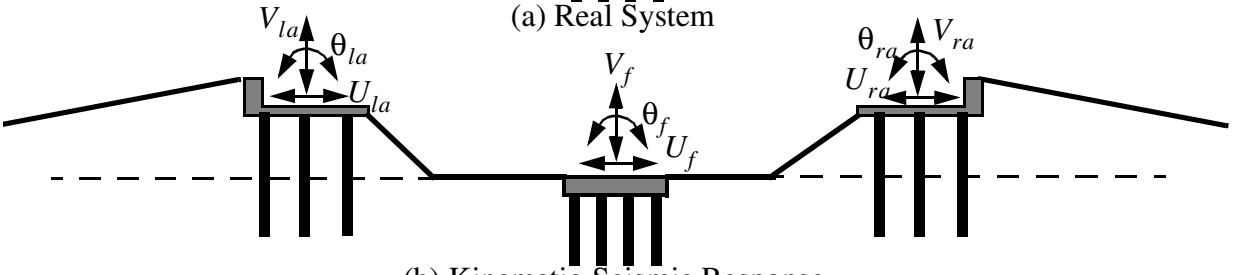

(b) Kinematic-Seismic Response

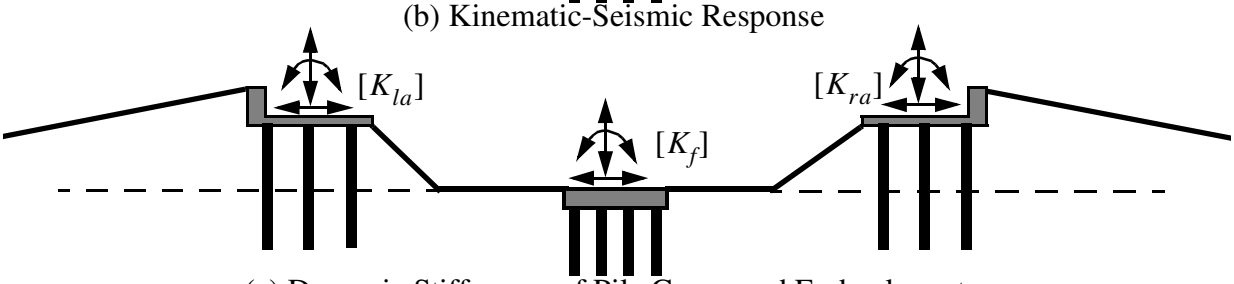

(c) Dynamic Stiffnesses of Pile Group and Embankments

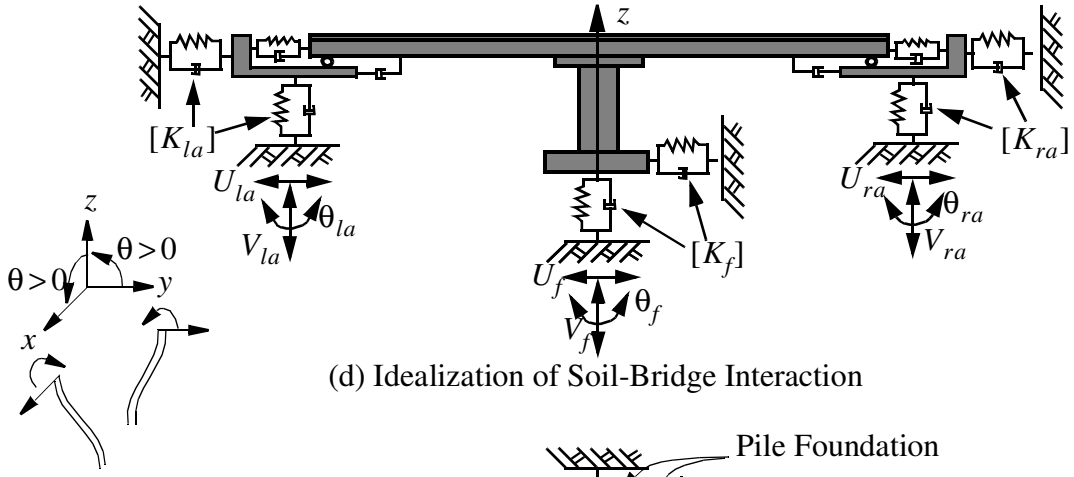

(d) Idealization of Soil-Bridge Interaction

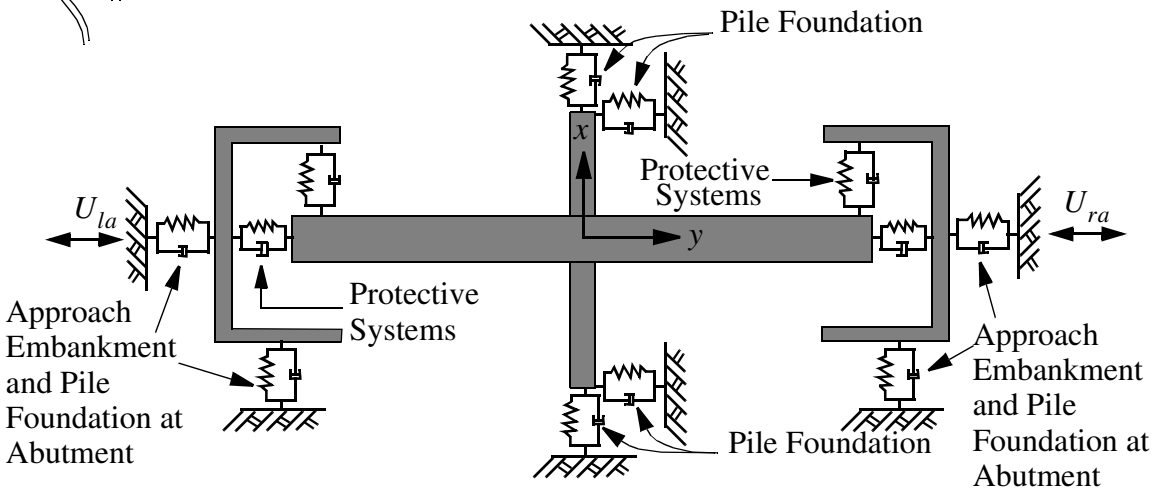

(e) Plan View of Idealized Model

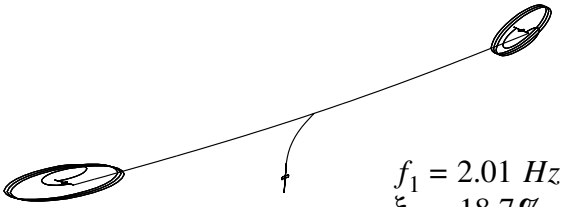

$f_1 = 2.01\ Hz$
$\xi_1 = 18.7\%$

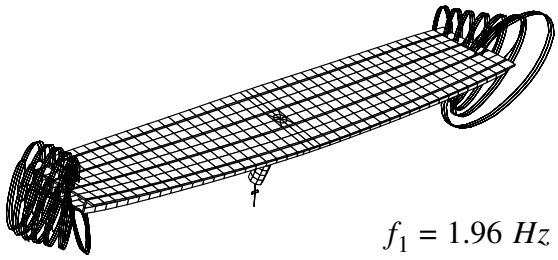

$f_1 = 1.96\ Hz$

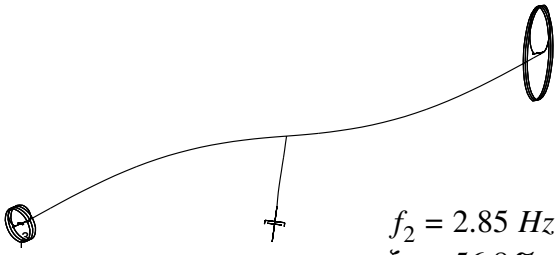

$f_2 = 2.85\ Hz$
$\xi_2 = 56.8\%$

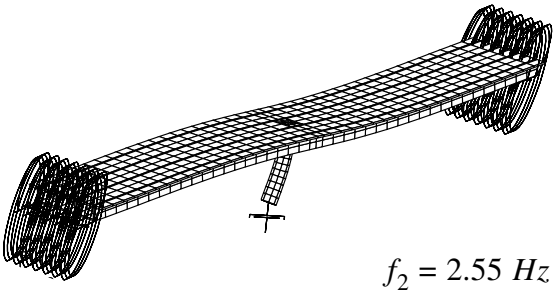

$f_2 = 2.55\ Hz$

$f_3 = 3.58\ Hz$
$\xi_3 = 8.3\%$

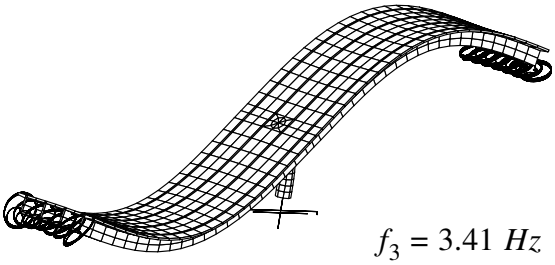

$f_3 = 3.41\ Hz$

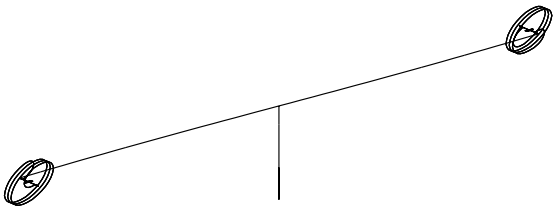

$f_4 = 4.00\ Hz$

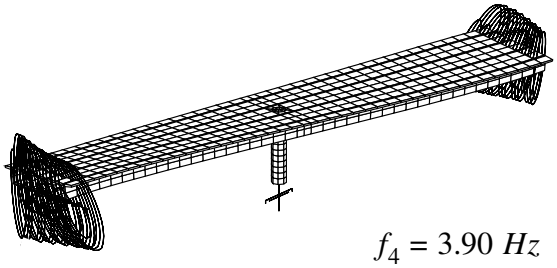

$f_4 = 3.90\ Hz$

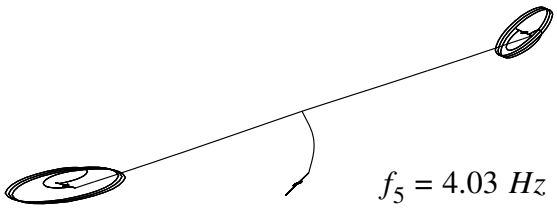

$f_5 = 4.03\ Hz$
$\xi_5 = 28.2\%$

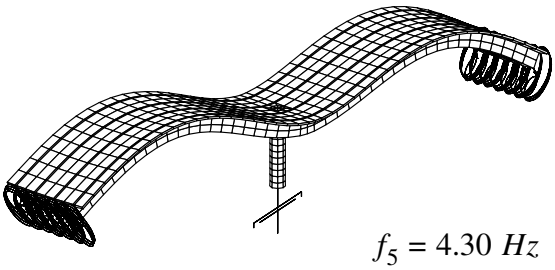

$f_5 = 4.30\ Hz$

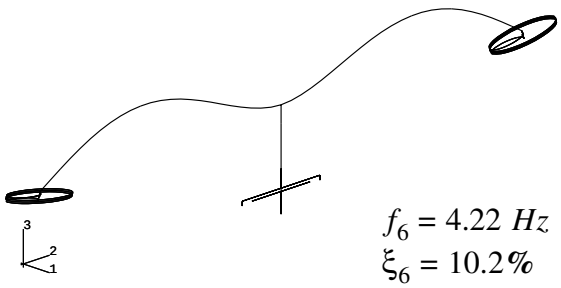

$f_6 = 4.22\ Hz$
$\xi_6 = 10.2\%$

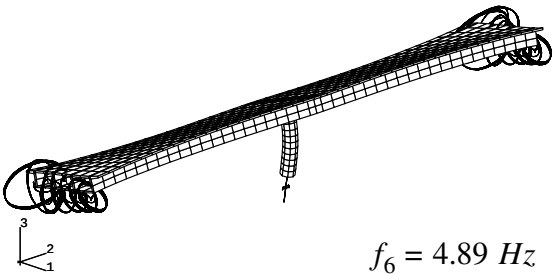

$f_6 = 4.89\ Hz$

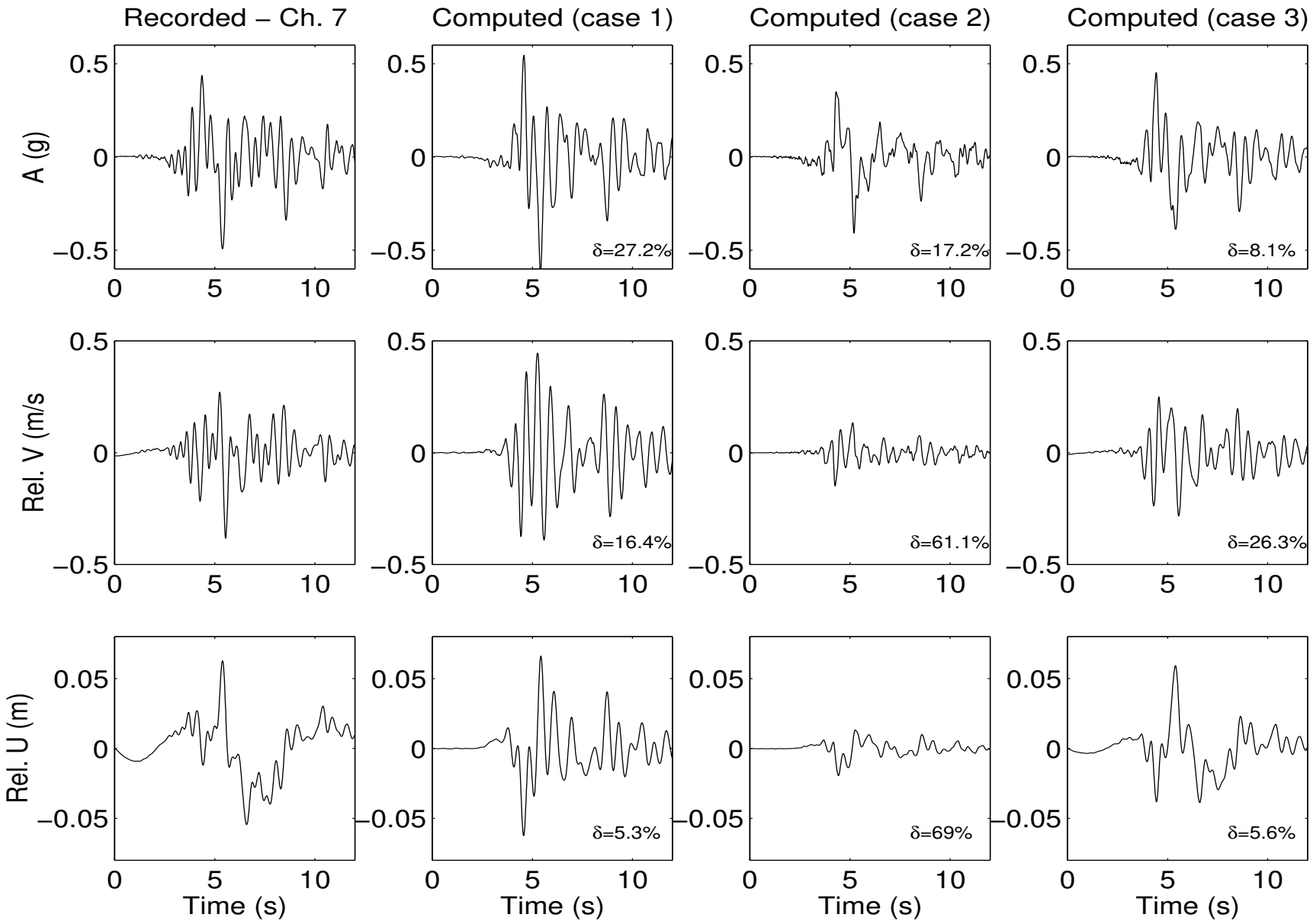
Recorded – Ch. 7
Computed (case 1)
Computed (case 2)
Computed (case 3)
A (g)
Rel. V (m/s
Rel. U (m)
Time (s)
δ=27.2%
δ=17.2%
δ=8.1%
δ=16.4%
δ=61.1%
δ=26.3%
δ=5.3%
δ=69%
δ=5.6%

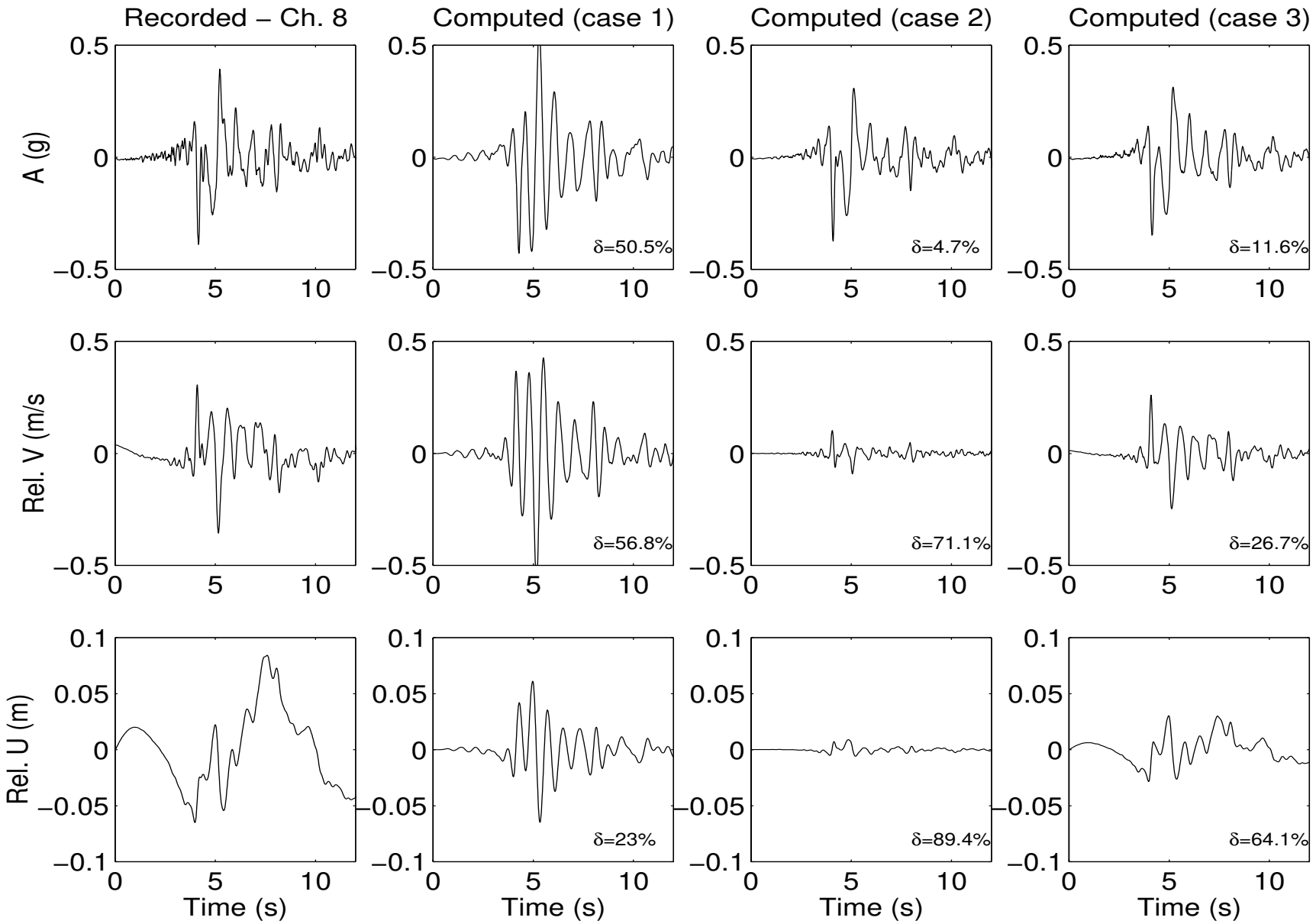
Recorded – Ch. 8
Computed (case 1)
Computed (case 2)
Computed (case 3)
A (g)
Rel. V (m/s
Rel. U (m)
δ=50.5%
δ=4.7%
δ=11.6%
δ=56.8%
δ=71.1%
δ=26.7%
δ=23%
δ=89.4%
δ=64.1%
Time (s)

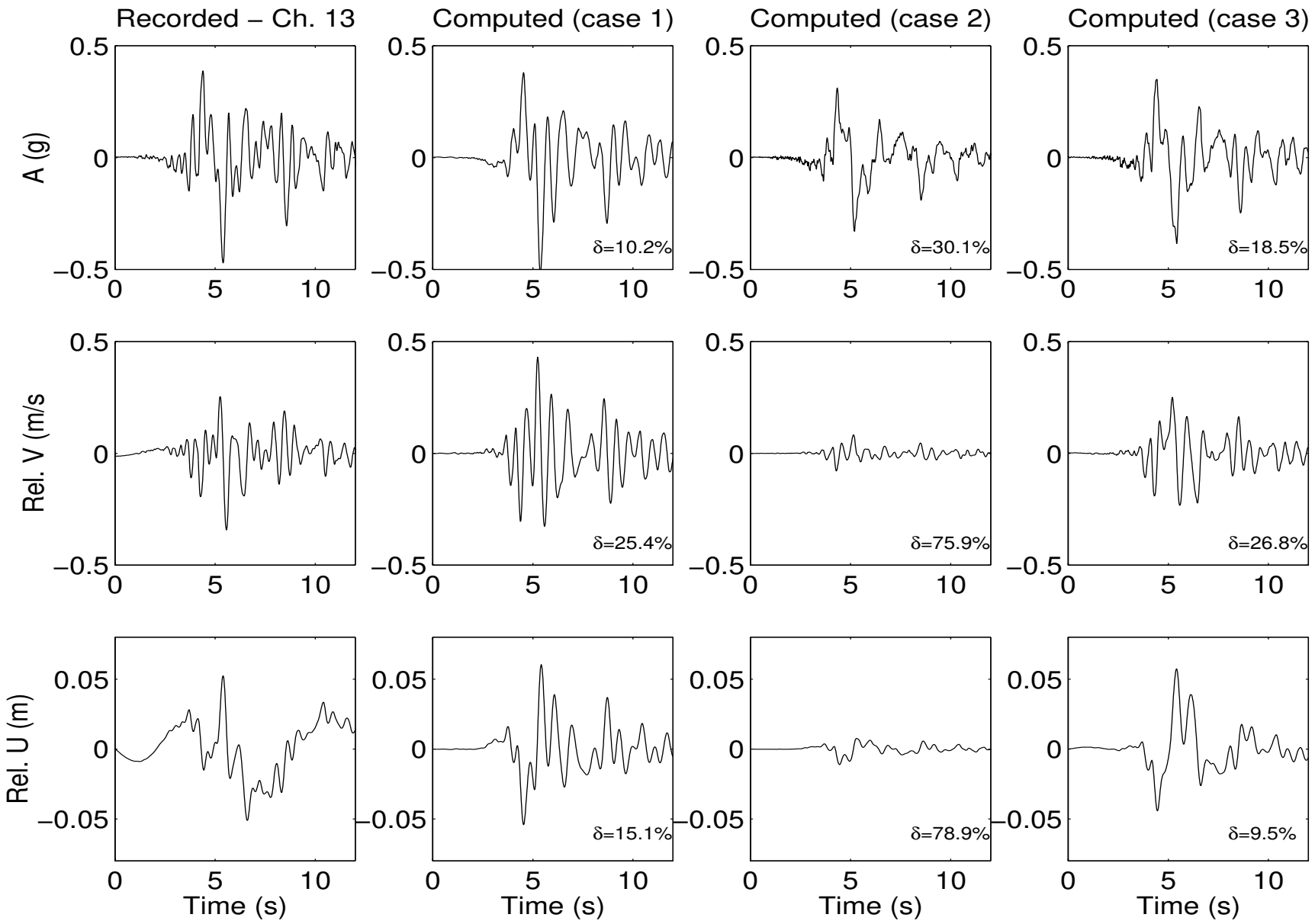
Recorded – Ch. 13
Computed (case 1)
Computed (case 2)
Computed (case 3)
A (g)
Rel. V (m/s
Rel. U (m)
δ=10.2%
δ=30.1%
δ=18.5%
δ=25.4%
δ=75.9%
δ=26.8%
δ=15.1%
δ=78.9%
δ=9.5%
Time (s)

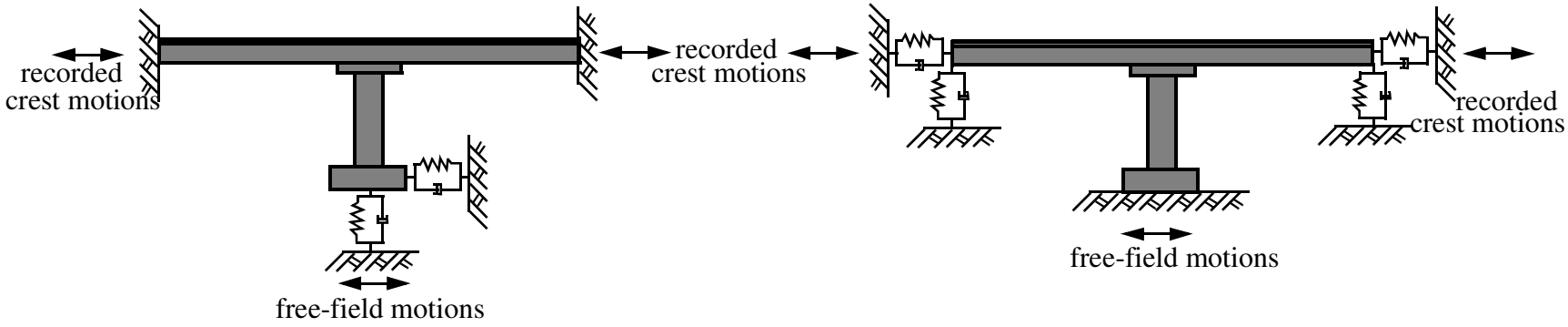

(a) Monolithic embankments and viscoelastic foundation at the center bent

(b) Viscoelastic embankments and monolithic support at the center bent

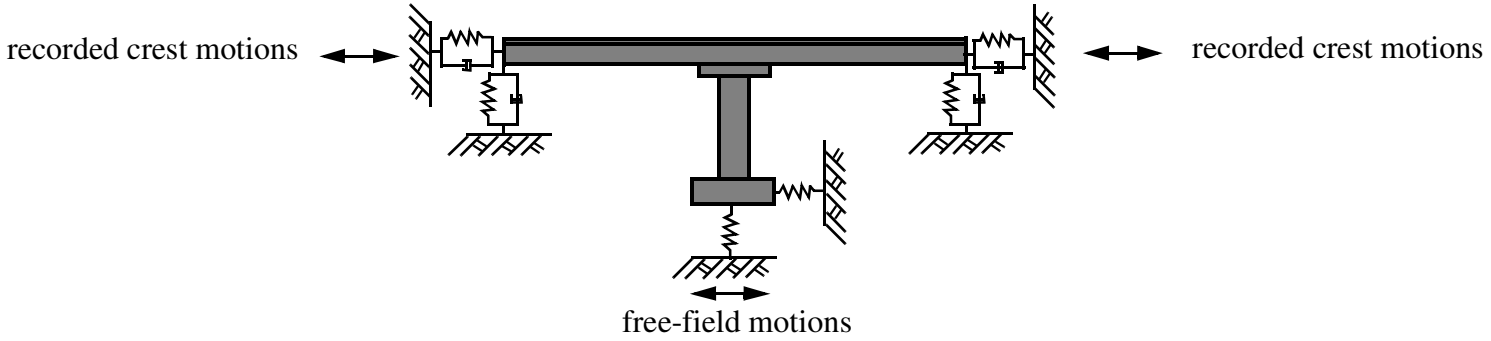

(c) Viscoelastic embankments and elastic support at the center bent

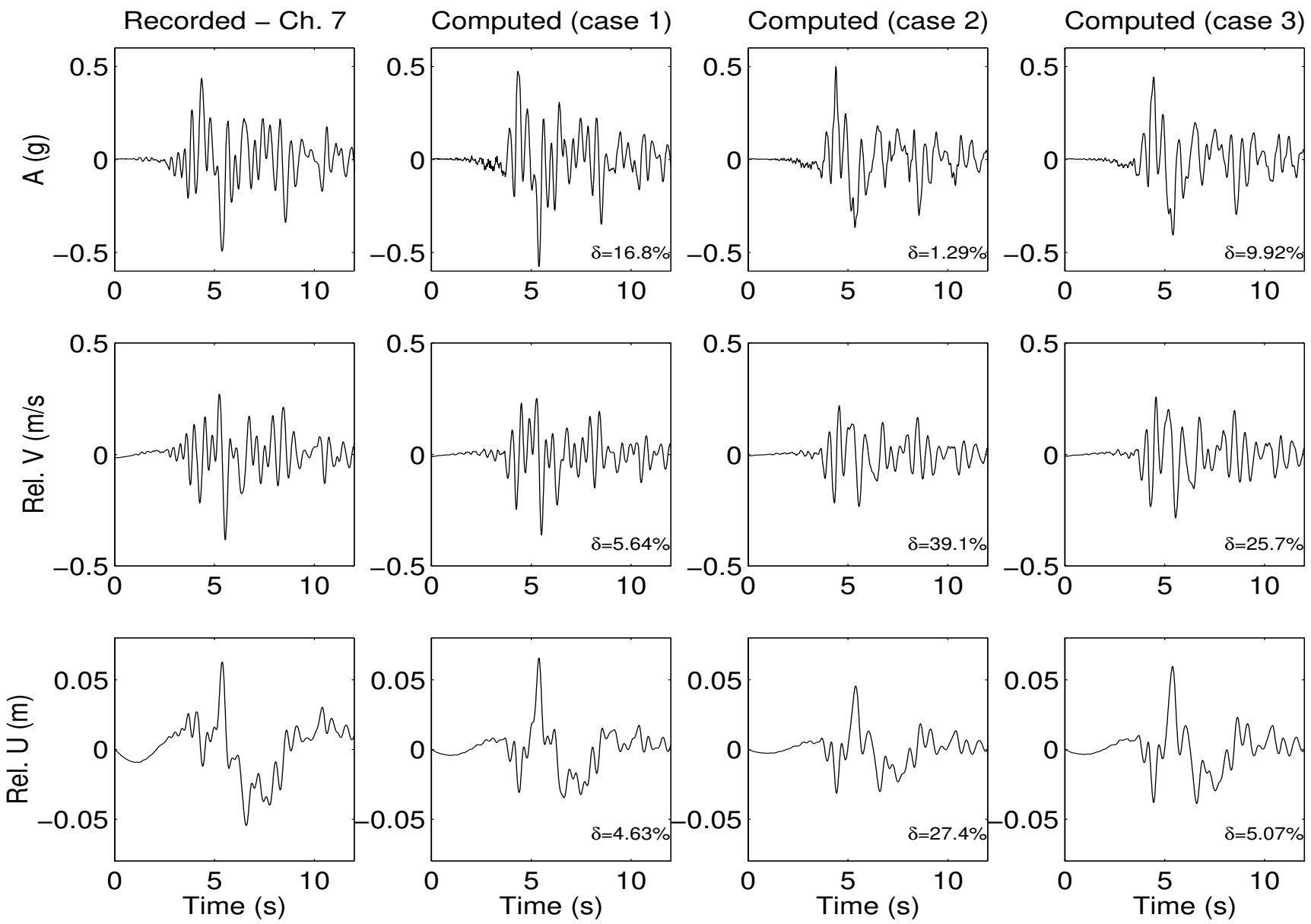
Recorded – Ch. 7
Computed (case 1)
Computed (case 2)
Computed (case 3)
A (g)
Rel. V (m/s
Rel. U (m)
δ=16.8%
δ=1.29%
δ=9.92%
δ=5.64%
δ=39.1%
δ=25.7%
δ=4.63%
δ=27.4%
δ=5.07%
Time (s)

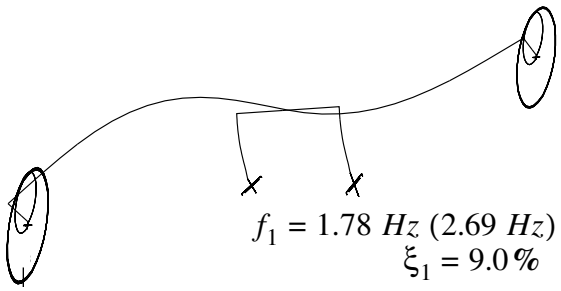

f_1 = 1.78 *Hz* (2.69 *Hz*)
ξ_1 = 9.0%

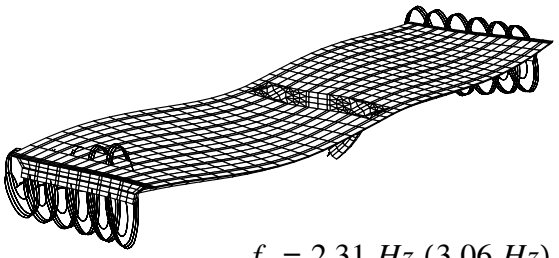

f_1 = 2.31 *Hz* (3.06 *Hz*)

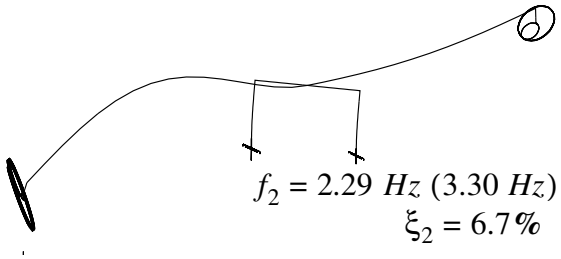

f_2 = 2.29 *Hz* (3.30 *Hz*)
ξ_2 = 6.7%

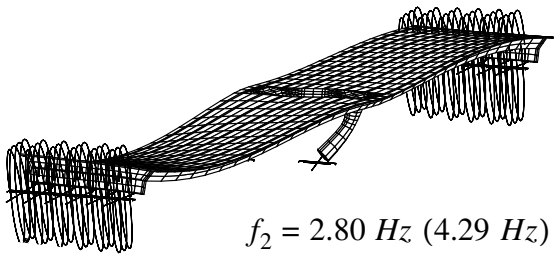

f_2 = 2.80 *Hz* (4.29 *Hz*)

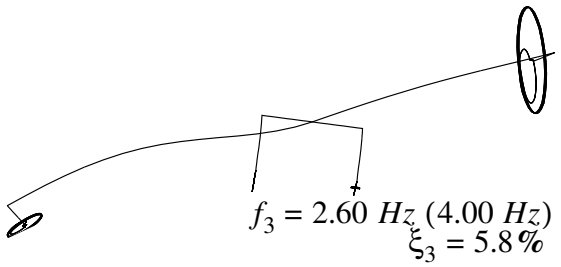

f_3 = 2.60 *Hz* (4.00 *Hz*)
ξ_3 = 5.8%

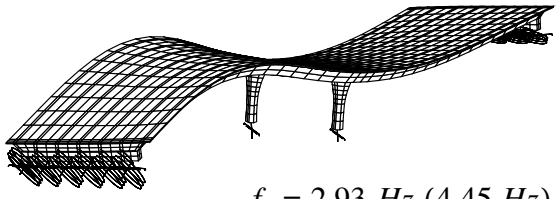

f_3 = 2.93 *Hz* (4.45 *Hz*)

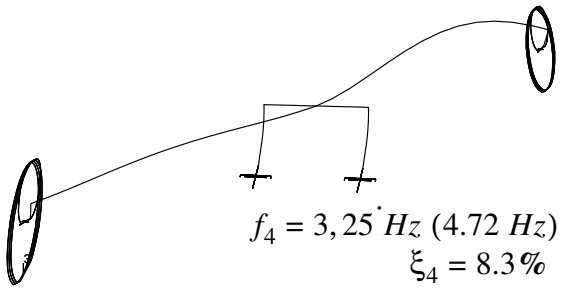

f_4 = 3,25 *Hz* (4.72 *Hz*)
ξ_4 = 8.3%

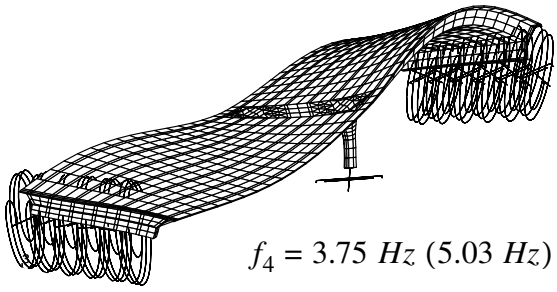

f_4 = 3.75 *Hz* (5.03 *Hz*)

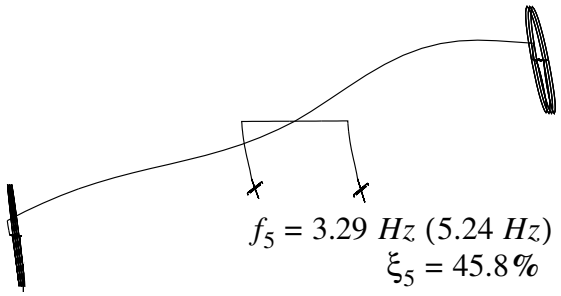

f_5 = 3.29 *Hz* (5.24 *Hz*)
ξ_5 = 45.8%

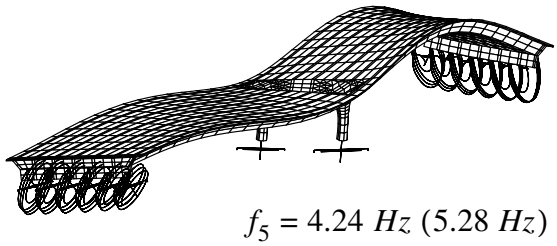

f_5 = 4.24 *Hz* (5.28 *Hz*)

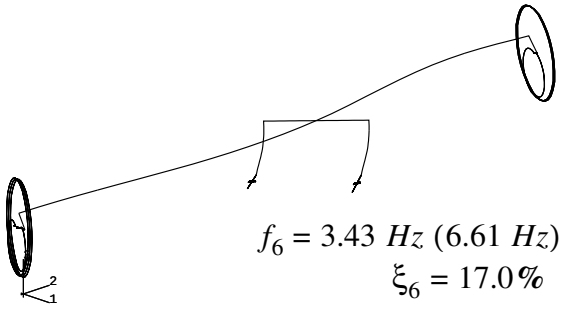

f_6 = 3.43 *Hz* (6.61 *Hz*)
ξ_6 = 17.0%

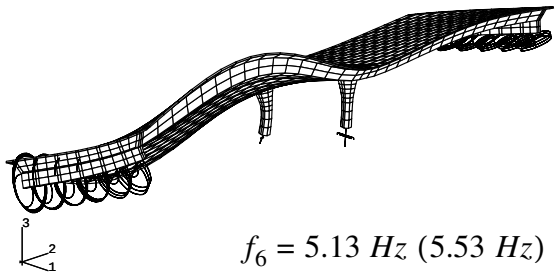

f_6 = 5.13 *Hz* (5.53 *Hz*)

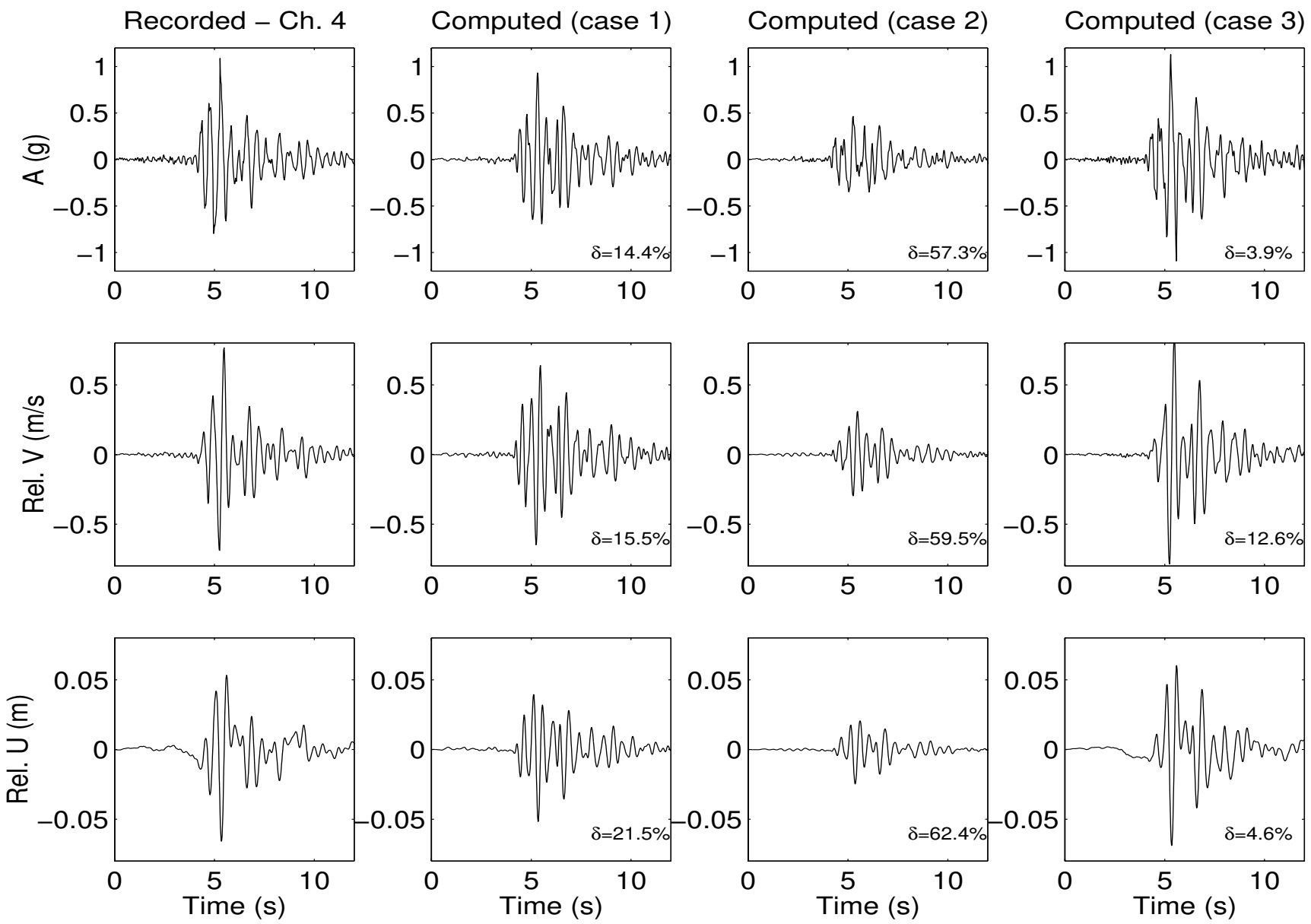
Recorded – Ch. 4
Computed (case 1)
Computed (case 2)
Computed (case 3)
A (g)
Rel. V (m/s
Rel. U (m)
δ=14.4%
δ=57.3%
δ=3.9%
δ=15.5%
δ=59.5%
δ=12.6%
δ=21.5%
δ=62.4%
δ=4.6%
Time (s)

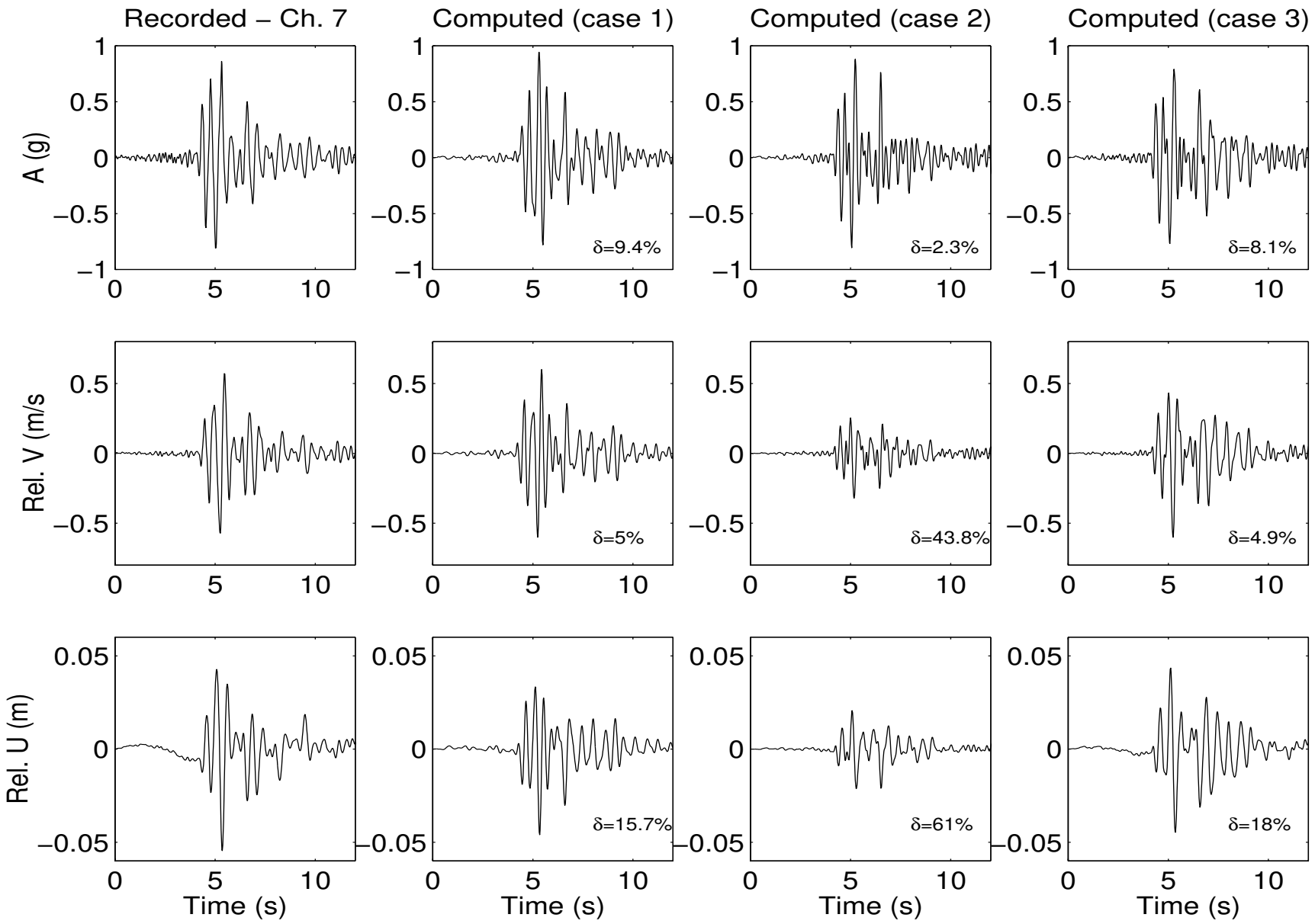
Recorded – Ch. 7
Computed (case 1)
Computed (case 2)
Computed (case 3)
A (g)
Rel. V (m/s
Rel. U (m)
Time (s)
δ=9.4%
δ=2.3%
δ=8.1%
δ=5%
δ=43.8%
δ=4.9%
δ=15.7%
δ=61%
δ=18%

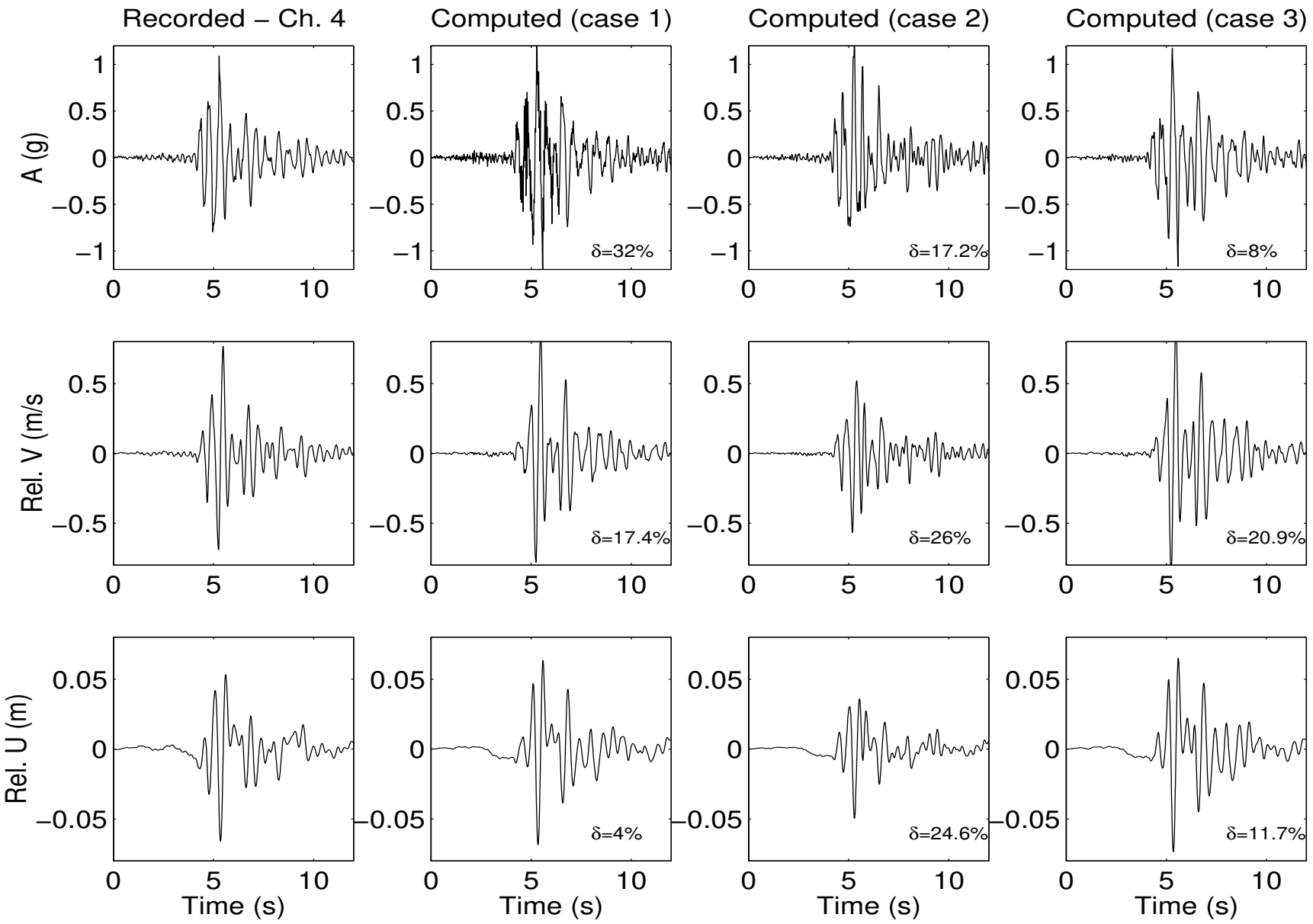
Recorded – Ch. 4
Computed (case 1)
Computed (case 2)
Computed (case 3)
A (g)
Rel. V (m/s
Rel. U (m)
δ=32%
δ=17.2%
δ=8%
δ=17.4%
δ=26%
δ=20.9%
δ=4%
δ=24.6%
δ=11.7%
Time (s)

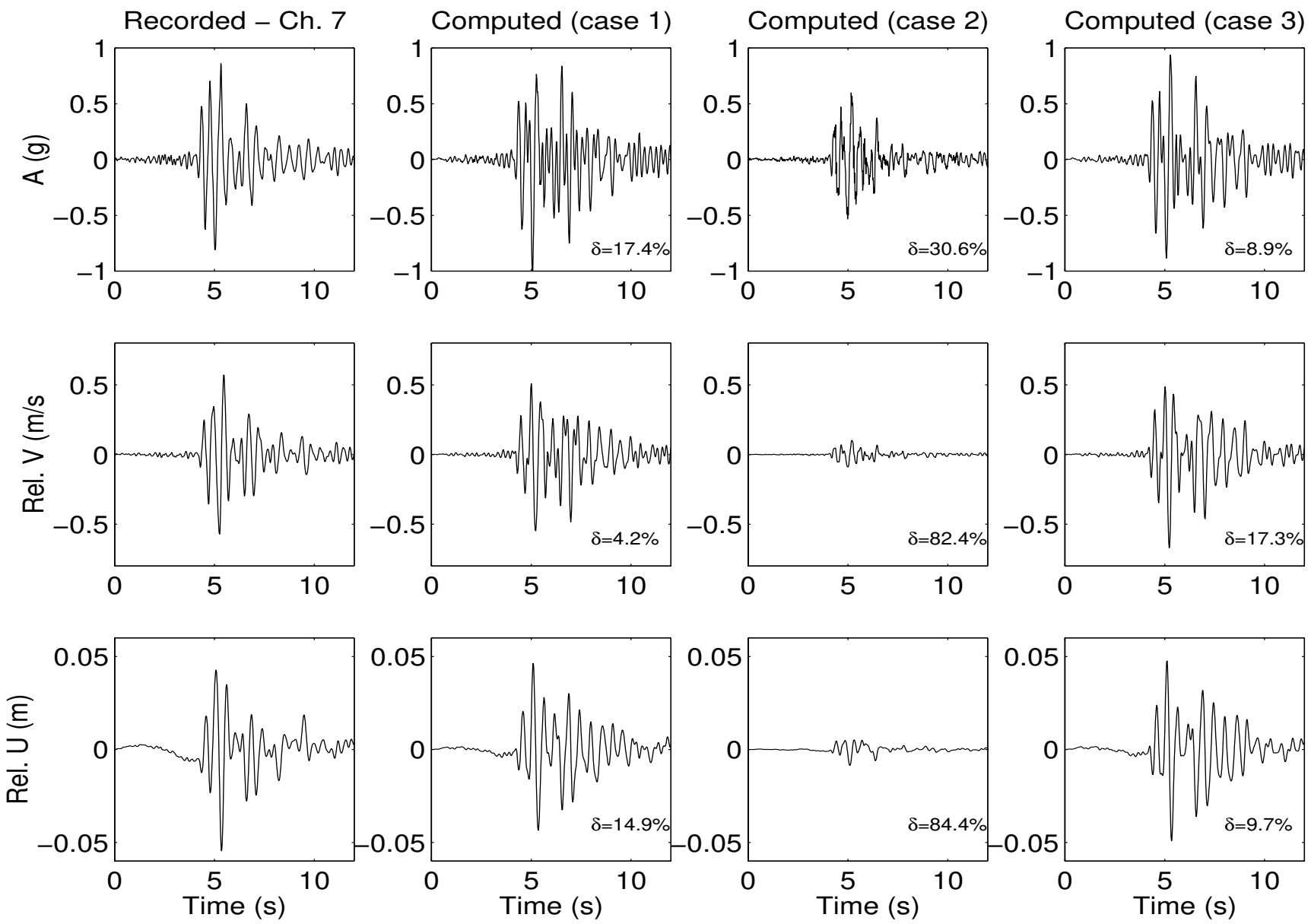
Recorded – Ch. 7
Computed (case 1)
Computed (case 2)
Computed (case 3)
A (g)
Rel. V (m/s
Rel. U (m)
δ=17.4%
δ=30.6%
δ=8.9%
δ=4.2%
δ=82.4%
δ=17.3%
δ=14.9%
δ=84.4%
δ=9.7%
Time (s)